Contents lists available at SciOpen

Food Science and Human Wellness

journal homepage: https://www.sciopen.com/journal/2097-0765

China Food Publishing Co.

Intestinal anti-inflammatory effect of a plant sterol food supplement in experimental murine colitis and cell co-culture models

Mussa Makran[a], Antonio Cilla[a,*], Rosa María Giner[b], María Carmen Recio[b], Luisa Tesoriere[c], Alessandro Attanzio[c], Guadalupe Garcia-Llatas[a]

[a] *Nutrition and Food Science Area, Faculty of Pharmacy and Food Sciences, University of Valencia, Valencia 46100, Spain*
[b] *Department of Pharmacology, Faculty of Pharmacy and Food Sciences, University of Valencia, Valencia 46100, Spain*
[c] *Department of Biological, Chemical and Pharmaceutical Sciences and Technologies, University of Palermo, Palermo 90123, Italy*

ARTICLE INFO

Article history:
Received 11 March 2024
Received in revised form 2 April 2024
Accepted 24 April 2024

Keywords:
Animal model
Antioxidant
Inflammatory bowel disease
Phytosterols
Ulcerative colitis

ABSTRACT

The potential of a plant sterol food supplement (PS-FS) in addressing intestinal inflammation *in vivo* and *in vitro* was evaluated. As *in vivo* model, C57BL/6J mice were exposed to 1.5% dextran sulfate sodium in three 5-day periods, with 10-day rest intervals in between, daily reciving PS-FS (35 mg PS/kg body weight). The *in vitro* approach involved a bi-cameral system with 8-day-differentiated Caco-2 (apical) and RAW264.7 cells (basolateral). The bioaccessible fraction of PS-FS, obtained after INFOGEST 2.0 simulated gastrointestinal digestion, was added to the apical part (90 min), followed by stimulation with lipopolysaccharide (1 μg/mL, 24 h). PS-FS alleviated rectal bleeding and rebalanced pro- (tumor necrosis factor α, interleukin (IL)-6, and IL-8) and anti-inflammatory cytokines (IL-10). Additionally, PS-FS ameliorated histopathological damage and enhancing occludin expression. A reduction in oxidative stress was evidenced by decreased myeloperoxidase activity and reactive oxygen species production. The anti-inflammatory mechanism included suppressing cyclooxygenase 2 expression, reducing prostaglandin E_2 production, and inhibiting the phosphorylation and nuclear translocation of the nuclear factor κB p65 subunit. This study reveals the potential of PS-FS as a therapeutic intervention for colitis. The alignment between *in vivo* and *in vitro* outcomes substantiates the appropriateness of the co-culture model to evaluate the anti-inflammatory activity of foods.

1. Introduction

Inflammatory bowel disease (IBD), which encompasses ulcerative colitis and Crohn's disease as representative phenotype, poses a challenge to global health systems due to its increasing incidence[1]. The management of this group of diseases involves pharmacological therapies such as anti-inflammatories, antibiotics and other biological agents, or even surgery in critically ill patients[2]. Despite advances in medical interventions, a substantial proportion of IBD patients continue to deal with inadequate control of their symptoms or report severe side effects to pharmacological treatments. This underscores the appeal of exploring pioneering therapeutic avenues, such as dietary bioactive compounds. Among these, plant sterols (PS), widely recognized for their ability to lower serum cholesterol, stand out for having demonstrated anti-inflammatory properties at the intestinal level[3]. Numerous investigations, using both *in vitro*[4-12] and *in vivo*[9-18] models of intestinal inflammation, have shown that PS safeguarding against colon shortening, mitigate histopathological impairments, and

* Corresponding author at: Nutrition and Food Science Area, Faculty of Pharmacy and Food Sciences, University of Valencia, Valencia 46100, Spain.
E-mail address: antonio.cilla@uv.es (A. Cilla)
Peer review under responsibility of Beijing Academy of Food Sciences.

SciOpen Publishing services by Tsinghua University Press

http://doi.org/10.26599/FSHW.2024.9250295

alleviate clinical manifestations. Despite the accumulating evidence, certain fundamental facets remain unexplored (e.g., effect on intestinal barrier function) and need to be addressed. Furthermore, the predominant research evaluates the therapeutic efficacy of PS in improving intestinal inflammation, while sparse data address its preventive capabilities.

Ethical implications associated with the use of animal models in research have raised significant criticism. Consequently, there has been a marked increase in efforts to identify alternatives that reduce the use of animals in experimentation, refine their methodologies and, whenever possible, replace them[19]. *In vitro* models based on cell cultures represent the best experimental approach to replace and reduce the number of experimental animals used in the evaluation of the anti-inflammatory potential of food and its components. However, cell models have limitations, as they are a simplified representation of the biological environment of living organisms, lacking the cellular diversity, tissue interactions, and systemic responses present in complex organisms[20]. To combat these limitations, more complex models have been proposed, the co-culture of cell lines being among the most used. In the context of the intestinal inflammation, an *in vitro* model has been developed to evaluate the anti-inflammatory effect of foods by establishing a co-culture system wherein Caco-2 intestinal epithelial cells were positioned on the apical side of Transwell® plate, while RAW264.7 macrophages occupied the basolateral side[21]. This configuration seeks to mimic the natural arrangement of intestinal components, reflecting the juxtaposition of the epithelial cells and the underlying immune cells scattered within the lamina propria. Facilitated by a porous membrane, this system facilitates cross-communication between the two distinct cell types, allowing the effect of these interactions on the resulting immune response to be explored. Until now, there are numbers of studies that have used this model (none with PS), although the data provided by it has not been verified using *in vivo* data. In this sense, animal models are considered as gold standard to validate *in vitro* models since they represent the best experimental approach. Among animal models of intestinal inflammation, colitis induced by dextran sulfate sodium (DSS) is the most appropriate model for verification of *in vitro* data since it has been used to describe both the study of the pathogenesis of ulcerative colitis and to evaluate the effectiveness of therapies[22].

The objective of this research was to evaluate the efficacy of a PS food supplement (PS-FS) in mitigating intestinal inflammation, elucidate its mechanism of action, and investigate specific facets of IBD that had not been explored before with PS such as intestinal barrier integrity. To accomplish this goal, a combined *in vivo-in vitro* methodology was employed, utilizing the well-established animal murine model of DSS-induced ulcerative colitis alongside a co-culture of Caco-2 and RAW264.7 cells. By assessing the effectiveness of PS-FS in both models, the aim was to validate and confirm the utility of the cell co-culture model for studying the anti-inflammatory effects of food products.

2. Material and methods

2.1 Dosage information

The PS-FS was composed by a commercially available microencapsulated free PS ingredient (Lipophytol® P Dispersable), employing as a control a PS-free placebo containing solely the excipients (both provided by Lipofoods, Barcelona, Spain). The PS content in the PS-FS was characterized as previously described[23]: β-sitosterol (60.7 ± 0.8)%; sitostanol (15.9 ± 0.7)%; campesterol (6.7 ± 0.3)%; campestanol (2.0 ± 0.1)%; Δ^7-stigmastenol (0.51 ± 0.02)%; stigmasterol (0.48 ± 0.02)%; Δ^7-avenasterol (0.33 ± 0.01)%; $\Delta^{5,24}$-stigmastadienol (0.247 ± 0.003)%; Δ^5-avenasterol (0.085 ± 0.004)%; total PS (86.8 ± 1.8)%. In addition, analysis of the PS-FS was carried out in terms of physical attributes (appearance, color, odor and density), presence of heavy metals (lead, arsenic, mercury and cadmium), and microbiological quality to achieve food grade standard. An aqueous suspension of PS-FS was prepared to administer the daily dose of 35 mg PS/kg body weight to the mice via intragastric gavage in accordance to a previous study[15].

2.2 Mice model of colitis

The ulcerative colitis model was established according to established protocols[22]. Female C57BL/6J mice (n = 34, 8 weeks old, 18–20 g body weight) were obtained from Envigo (Indianapolis, IN, USA) and placed in environmentally controlled room (22 ℃, 60% relative humidity and 12-h/12-h light/dark cycle) with free access to autoclaved chow and water. After an acclimatization 7-day period, mice were randomized into 6 groups (Fig. 1). Two groups served as healthy controls (3 mice/group) and received daily placebo or PS-FS. Additionally, 4 groups (7 mice/group) were exposed to 1.5 g/100 mL DSS (48 kDa; MP Biomedicals, Irvine, CA, USA) in drinking water for three 5-day periods, with 10-day rest intervals in between,

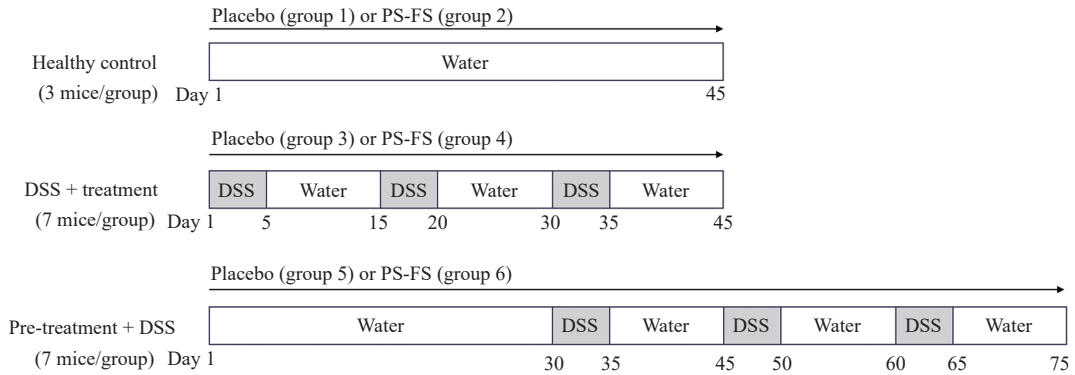

Fig. 1 Experimental design of animal study. Control groups (i.e., non-DSS exposed mice) received daily placebo or PS-FS (35 mg PS/kg body weight). In the rest of the groups, colitis was chemically-induced by DSS, and the administration of placebo or PS-FS started either with the first exposure to DSS (treatment) or 30 days before (pre-treatment).

receiving placebo or PS-FS from the time they were first exposed to DSS (treatment) or 30 days before (pre-treatment).

2.3 Simulated digestion of PS-FS

To expose the cell culture to the PS-FS under conditions close to gastrointestinal physiology, the PS-FS was subjected to simulated gastrointestinal digestion. An aqueous suspension was prepared by adding the dose of 2 g PS (equivalent to 2.3 g of PS-FS according to the purity) to 200 mL of water, in accordance with the customary approach for ingesting powdered supplements. Subsequently, 5 mL of this suspension (or water for digestion blank) were digested following the INFOGEST 2.0 harmonized method adapted to PS[24]. The digesta was centrifuged (3 100 × *g*, 4 °C for 90 min) to obtain the bioaccessible fraction (BF), which was subsequently sterilized by filtration (0.22 µm). The PS concentration in BF was quantified using a previously established method[24]: *β*-sitosterol (185.5 ± 4.6) µmol/L; sitostanol (51.6 ± 1.3) µmol/L; campesterol (12.5 ± 0.6) µmol/L; campestanol (7.6 ± 0.0) µmol/L; Δ^7-stigmastenol (0.7 ± 0.1) µmol/L; stigmasterol (0.9 ± 0.1) µmol/L; Δ^7-avenasterol (0.6 ± 0.1) µmol/L; $\Delta^{5,24}$-stigmastadienol (0.68 ± 0.01) µmol/L; Δ^5-avenasterol (0.37 ± 0.04) µmol/L; total PS (260.4 ± 6.7) µmol/L.

2.4 In vitro co-culture model of intestinal inflammation

Caco-2 and RAW264.7 cells were purchased from American Type Culture Collection (HTB-37 and TIB-71, respectively; Rockville, MD, USA). Both cell lines were cultured in DMEM high glucose (4.5 g/L glucose) supplemented with 10% (*V*/*V*) fetal bovine serum, 100 U/mL penicillin and 100 µg/mL streptomycin (Euroclone, Milan, Italy). Cells were incubated at 37 °C in a controlled humid environment (95% relative humidity) with 5% (*V*/*V*) CO_2. For experimental study (graphically represented in Fig. 2), Caco-2 cells were seeded (9 × 10^4 cells/well) in the apical compartment of Transwell® plates (1.12 cm^2 membrane area, 0.4 µm pore size; Corning CoStar Corp., Cambridge, MA, USA) to a differentiated state (8 days), indicated by a transepithelial electrical resistance (800 Ω·cm^2)[5]. One day before finalizing the differentiation of Caco-2 cells, RAW264.7 macrophages were seeded in a 12-well plate (3.4 × 10^5 cells/well) and were maintained for 24 h. Subsequently, Transwell® inserts containing the differentiated Caco-2 cells were placed into the 12-well plate pre-loaded with RAW264.7 macrophages. Then, 0.5 mL of culture medium or BF of PS-FS and digestion blank (diluted at 1:20 (*V*/*V*) to ensure no cytotoxic effects, as confirmed by MTT assay[25] testing of a range of dilutions from 1:2 to 1:30 (*V*/*V*)) were introduced into the apical compartment and incubated for 90 min. After the incubation, the BF was replaced with culture medium, and a pro-inflammatory stimulus was induced by addition 1 µg/mL of lipopolysaccharide (LPS) from *Escherichia coli* O127:B8 (Merck LifeScience S.L.U., Madrid, Spain) for 24 h in the basolateral chamber.

2.5 Evaluation of disease activity index (DAI) in mice model

During the experiment, body weight, stool consistency, and rectal bleeding were recorded. The DAI was scored at the end of the experiment, considering only the consistency of the feces (0: normal, 2: loose, 4: diarrhea) and rectal bleeding (0: no rectal blood observed, 2: slight bleeding, 4: gross bleeding), since the mice did not exhibit loss of body weight at this point. These two scores were combined, and the resulting sum was divided by 2[15].

2.6 Quantification of fecal lipocalin 2 (Lcn-2) in mice model

The non-invasive biomarker of intestinal inflammation, Lcn-2, was measured in fecal samples before and after DSS exposure of each cycle[26]. Fresh feces were collected, resuspended in phosphate buffered saline (PBS) containing 0.1% (*V*/*V*) Tween-20 and vortexed at 2 000 r/min for 20 min. The fecal suspension was clarified by

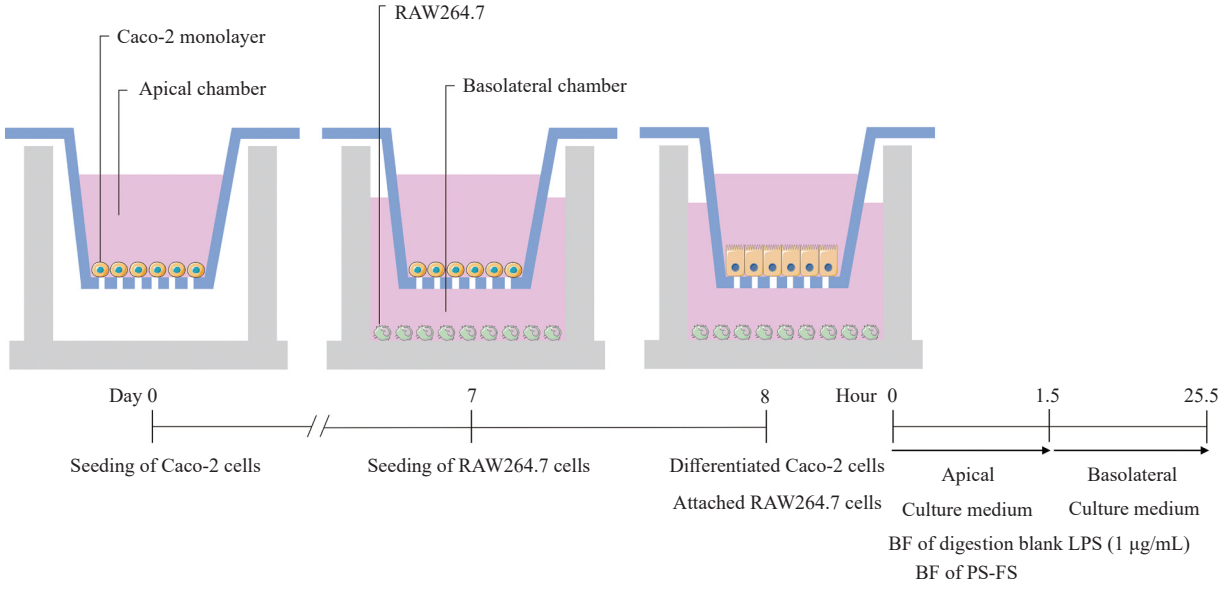

Fig. 2 Co-culture model of intestinal inflammation. Caco-2 and RAW264.7 cells were seeded in the apical and basolateral compartment, respectively, of 12-well Transwell® plates. Caco-2 cells were incubated for 8 days to cell differentiation, meanwhile, RAW264.7 cells were kept for 24 h to adhere to the well. The Caco-2 cells were exposed for 1.5 h to the culture medium (control cells) or BF of PS-FS or digestion blank. Then, a pro-inflammatory response was triggered by LPS in the basolateral compartment (1 µg/mL, 24 h).

centrifugation (14 000 × *g*, 4 °C for 10 min) and concentration of Lcn-2 was quantified in the supernatants using an enzyme linked immunosorbent assay (ELISA) kit following the manufacturer's instructions (R&D Systems, Minneapolis, MN, USA).

2.7 Analysis of edema and shortening of the colon

Mice were euthanized at days 45 (treatment) or 75 (pre-treatment) by cervical dislocation. The intestinal fragment of interest (ileocecal junction to anal verge) was removed and measured (length and weight). Before weighing, colon sections were thoroughly cleaned with PBS to remove fecal matter and thereby ensure accurate analysis of colon weight/length ratio. It was fragmented and immediately frozen (–80 °C) until analysis.

2.8 Histopathology analysis

Colon samples from mice were fixed in 4% (*V*/*V*) formalin overnight at room temperature, embedded in paraffin and sectioned at 4 µm. Sections were stained with hematoxylin and eosin (HE) and examined by Leica DMR light optical microscope (Leica, Wetzlar, Germany). Histopathological score was calculated by adding the score of the following parameters: crypt architecture (0–4: normal to severe crypt distortion with loss of surface epithelium), degree of inflammatory cell infiltration (0–3: normal to dense inflammatory infiltrate) and extent of inflammation (0–3: normal to transmural)[27].

2.9 Immunofluorescence analysis

Occludin expression was assessed by immunofluorescent staining in mice colon[28]. Paraffin-embedded formalin-fixed sections were depaaffinized, rehydrated and blocked with 2 g/100 mL bovine serum albumin for 1 h at room temperature. Then, colon sections were incubated with anti-occludin antibody (1:250, *V*/*V*) for overnight at 4 °C and then labeled with detection antibody (1:400, *V*/*V*) and DNA dye 4′,6-diamidino-2-phenylindole (DAPI; 1.5 µg/mL) (1 h at room temperature). Colon sections were observed using a confocal fluorescence microscope (Fluoview FV1000; Olympus, Tokyo, Japan). The signal intensity was quantified by ImageJ software (1.54d, National Institutes of Health, USA).

2.10 Analysis of myeloperoxidase (MPO) activity

MPO activity was measured in colonic tissue as an indicator of oxidative stress and neutrophil infiltration[29]. Colons were homogenized in 80 mmol/L sodium phosphate buffer (pH 5.4) containing 0.5 g/100 mL hexadecyltrimethylammonium bromide using a homogenizer (Polytron™ PT 2100, Kinematica® AG, Lucerne Switzerland) at 30 000 r/min for 3 min. Homogenates were centrifuged (12 000 × *g*, 4 °C for 15 min) and 100 µL of supernatant were loaded into a 96-well plate, with 100 µL of PBS, 15 µL of 0.017% (*V*/*V*) H_2O_2 and 20 µL of 18.5 mmol/L 3,3′,5,5′-tetramethylbenzidine. After incubation (20 min at 37 °C), absorbance at 630 nm was measured with a multiwell spectrophotometer (Victor3 multi-brand counter, Perkin-Elmer, Boston, MA, USA).

2.11 Determination of reactive oxygen species (ROS)

Intracellular levels of ROS in Caco-2 cells were measured using 2′,7′-dichlorofluorescein diacetate (DCFDA; Merck LifeScience S.L.U.)[30]. Briefly, 10 µL of whole-protein extract of Caco-2 cells (see Section 2.12) were incubated with 80 µL of PBS and 10 µL of 10 µmol/L DCFDA in a 96-well microtiter plate (30 min, 37 °C). Oxidation of DCFDA to its fluorescent product was measured by microplate reader (Promega GloMax®, Milan, Italy) with excitation/emission at 485 nm/535 nm. The measured fluorescence was normalized by total protein content.

2.12 Protein extraction

The methodology employed for protein extraction and Western blot was carried out following the previously described procedures[30]. Total protein content of protein extracts was quantified by Bradford's method[31].

2.12.1 Mice colon

Total proteins were extracted from colon homogenizing with lysis buffer containing 1% (*V*/*V*) Nonidet P-40, 0.5 g/100 mL sodium deoxycholate, 0.1 g/100 mL sodium dodecyl sulfate (SDS), 2 mmol/L phenylmethylsulfonyl fluoride, 1 mmol/L sodium orthovanadate and 1% (*V*/*V*) protease inhibitor cocktail (Santa Cruz Biotechnology Inc., Santa Cruz, CA, USA). Homogenates were clarified by centrifugation (15 000 × *g*, 4 °C for 15 min).

2.12.2 Caco-2 cells

Caco-2 cells were harvested from permeable membrane inserts and lysed with ice-cold buffer (50 mmol/L Tris-HCl (pH 7.4), 150 mmol/L NaCl, 1% (*V*/*V*) Triton X-100, 0.1 g/100 mL SDS, 1% (*V*/*V*) phosphatase inhibitor and 1% (*V*/*V*) protease inhibitor). After three freezing/thawing cycles, lysates were centrifuged (12 000 × *g*, 4 °C for 10 min) and the supernatants correspond to whole-cell protein extract.

2.12.3 RAW264.7 macrophages

Cells were lysed in hypotonic buffer (10 mmol/L 2-[4-(2-hydroxyethyl)piperazin-1-yl]ethanesulfonic acid (HEPES), 1.5 mmol/L $MgCl_2$, 10 mmol/L KCl, 0.1 mmol/L ethylene diamine tetraacetic acid (EDTA), 1% (*V*/*V*) phosphatase inhibitor and 1% (*V*/*V*) protease inhibitor), incubating 15 min in ice. The resulting lysate was centrifuged (12 000 × *g*, 4 °C for 20 min) to obtain the cytosolic fraction (supernatant). The pellet was lysed in nuclear extraction buffer (20 mmol/L HEPES, 25% (*V*/*V*) glycerol, 0.42 mmol/L NaCl, 1.5 mmol/L $MgCl_2$, 0.2 mmol/L EDTA, 0.1 mmol/L dithiothreitol, 1% (*V*/*V*) phosphatase inhibitor and 1% (*V*/*V*) protease inhibitor), incubating 30 min in ice. Finally, nuclear fraction was obtained by centrifugation (20 000 × *g* for 10 min at 4 °C).

2.13 ELISA assays

Cytokines with pro- (tumoral necrosis factor α (TNF-α) and interleukin (IL)-6) and anti-inflammatory activity (IL-10) were quantified in whole-tissue extract derived from colon by means of ELISA kits (Thermo Fisher Scientific, MA, USA). Additionally, the secretion of inflammatory mediators by Caco-2 and RAW264.7 cells was also assessed by quantifying their levels with ELISA kits in the apical (IL-8) or basolateral medium (TNF-α, IL-6, and prostaglandin E_2 (PGE_2)).

2.14 Western blot

Evaluation of the nuclear factor κB (NF-κB) pathway involved was analysed through the phosphorylation of the p65 subunit (resulting in p-p65) in the colon of mice and tracking its movement into the cell nucleus within RAW264.7 cells. Furthermore, the levels of cyclooxygenase 2 (COX-2) were quantified in both the complete colon tissue extract and the cytosolic fraction of RAW264.7 cells, and the occludin expression was evaluated in Caco-2 cells. For this purpose, equal amounts of protein (50 μg) were electrophoresed onto 7.5% SDS-polyacrylamide gel electrophoresis and electrotransferred to a polyvinylidene difluoride membrane. Membranes were blocked with 5% defatted milk in Tris-buffered saline with 0.05% (*V*/*V*) Tween-20 for 1 h at room temperature and incubated with primary antibodies (1:500, *V*/*V*) for overnight at 4 °C. Then, membranes were incubated (60 min at room temperature) with secondary antibody conjugated with fluorochrome (colon mice) (1:7 500, *V*/*V*) or horseradish peroxidase (cell culture) (1:2 000, *V*/*V*). Fluorescence was detected by Amersham ImageQuant 800 (Cytiva, Tokyo, Japan), while chemiluminescence was measured by iBright FL 1500 imaging system (Thermo Fisher Scientific, Waltham, MA, USA). After signal quantification by ImageJ software, data were normalized with β-actin (whole and cytosolic extract) or laminin B (nuclear fraction).

2.15 Statistical analysis

One-way analysis of variance (ANOVA), followed by post hoc HSD Tukey test, or *t*-test was applied to determine statistically significant differences ($P < 0.05$). Statgraphics Plus 5.1 software (Statpoint Technologies Inc., Warrenton, VA, USA) was used for statistical analysis. All experiments were conducted in two independent assays (at least $n = 3$).

3. Results

3.1 Clinical symptoms and anatomopathological analysis of colitis in mice

The clinical manifestations of a disease provide valuable information that helps to assess its severity and monitor the response to treatment. In the present study, the DSS-induced colitis model was clinically manifested by classic symptoms such as loss of body weight, loose stools, and rectal bleeding (Fig. 3). Treatment and pre-treatment with the PS-FS reduced (*vs*. DSS + placebo, $P < 0.05$) the clinical score of rectal bleeding (by 58% and 44%, respectively), which led to a lower DAI (by 40% and 27%, respectively). Nevertheless, PS-FS failed to improve weight loss and stool consistency.

On the other hand, during the inflammatory process in the colon, phenomena such as fibrosis (i.e., the formation of scar tissue) of the intestine and increased permeability of blood vessels occur, which causes a decrease in the length of the colon and favors its swelling[22]. These anatomopathological features were observed in the present study in mice exposed to DSS and were not alleviated by PS-FS treatment (Fig. 4). However, pre-treatment with PS-FS prevented the appearance of edema, without affecting colon shortening.

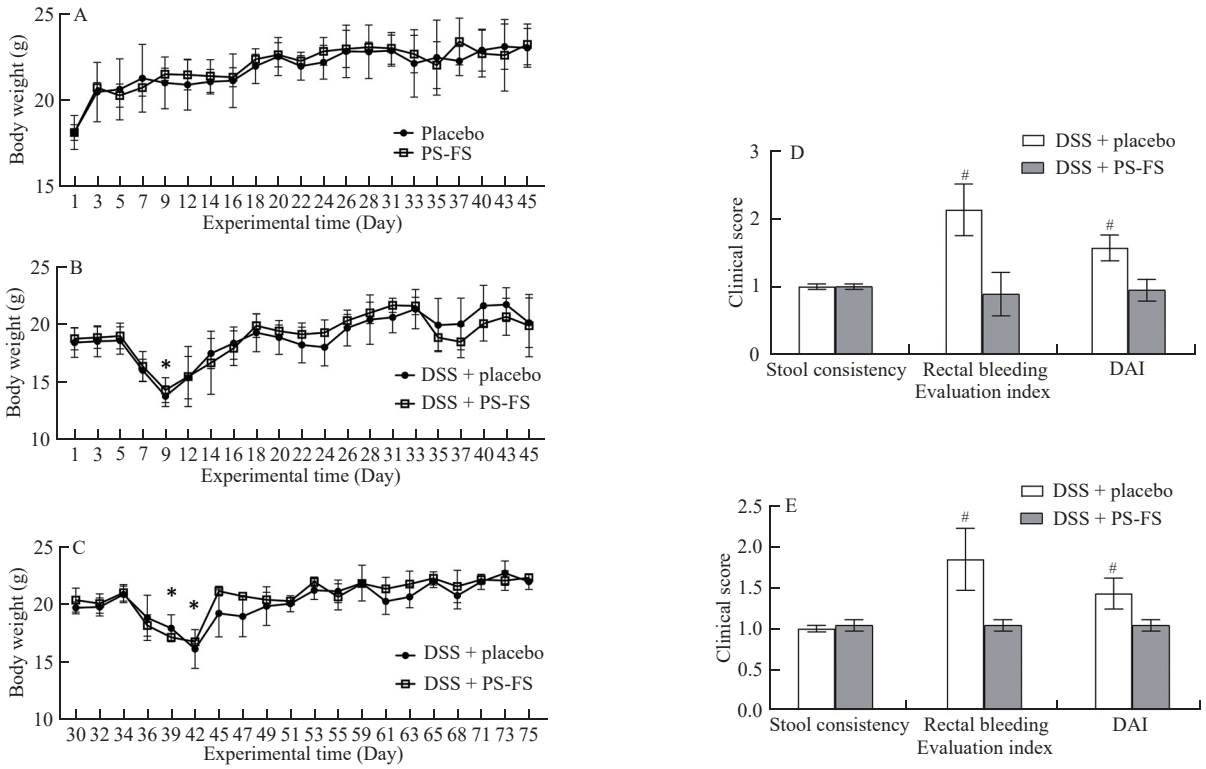

Fig. 3 Body weight evolution of mice of (A) control group and mice exposed to DSS and receiving placebo or PS-FS, (B) from the time of first exposition to DSS (treatment) or (C) 30 days before (pre-treatment). Clinical score on (D) days 45 (treatment) or (E) 75 (pre-treatment). Control mice did not manifest any of these symptoms and therefore data are not shown. Statistically significant differences ($P < 0.05$) in body weight from baseline in the same group (*) or clinical score between the placebo and PS-FS groups ($^{\#}$) are indicated.

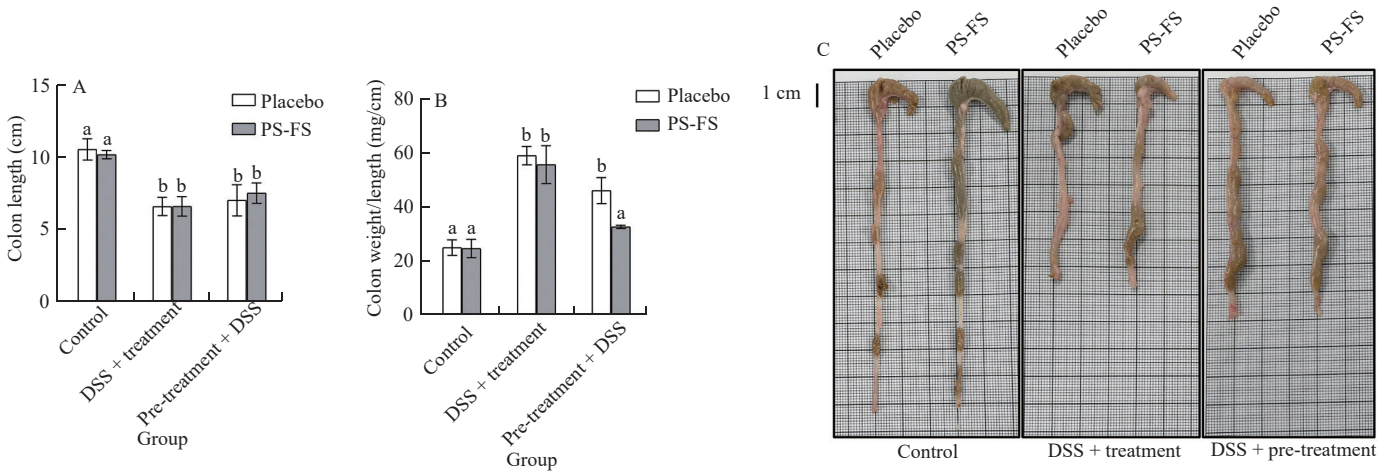

Fig. 4 (A) Length, (B) weight/length ration and (C) appearance of colon in control mice or DSS exposed mice receiving placebo or PS-FS, from the time of first exposition to DSS (treatment) or 30 days before (pre-treatment). Different letters (a–b) indicate statistically significant difference ($P < 0.05$) between groups.

3.2 Histopathology and intestinal barrier function

Staining with HE of colonic tissue allow the examination of structural changes, tissue organization, and inflammatory patterns. However, due to its limitations, it is advisable to use complementary techniques to further analyze the structure of the colon. In the context of colitis, it is particularly valuable to evaluate the expression of proteins that form tight junctions between epithelial cells. In the present study, histological analysis revealed severe inflammation in the mucosa and submucosa of the colon of mice exposed to DSS, manifested by a profuse infiltration of immune cells, loss of epithelial architecture and damage to the crypts (Fig. 5A). In addition, DSS exposure resulted in a significant reduction (*vs.* healthy control, $P < 0.05$) of the occludin expression (Fig. 5B). Treatment with PS-FS did not improve the histopathological damage induced by DSS in the colon, although it raised occludin expression 1.7-fold (*vs.* DSS + placebo, $P < 0.05$). However, the greatest

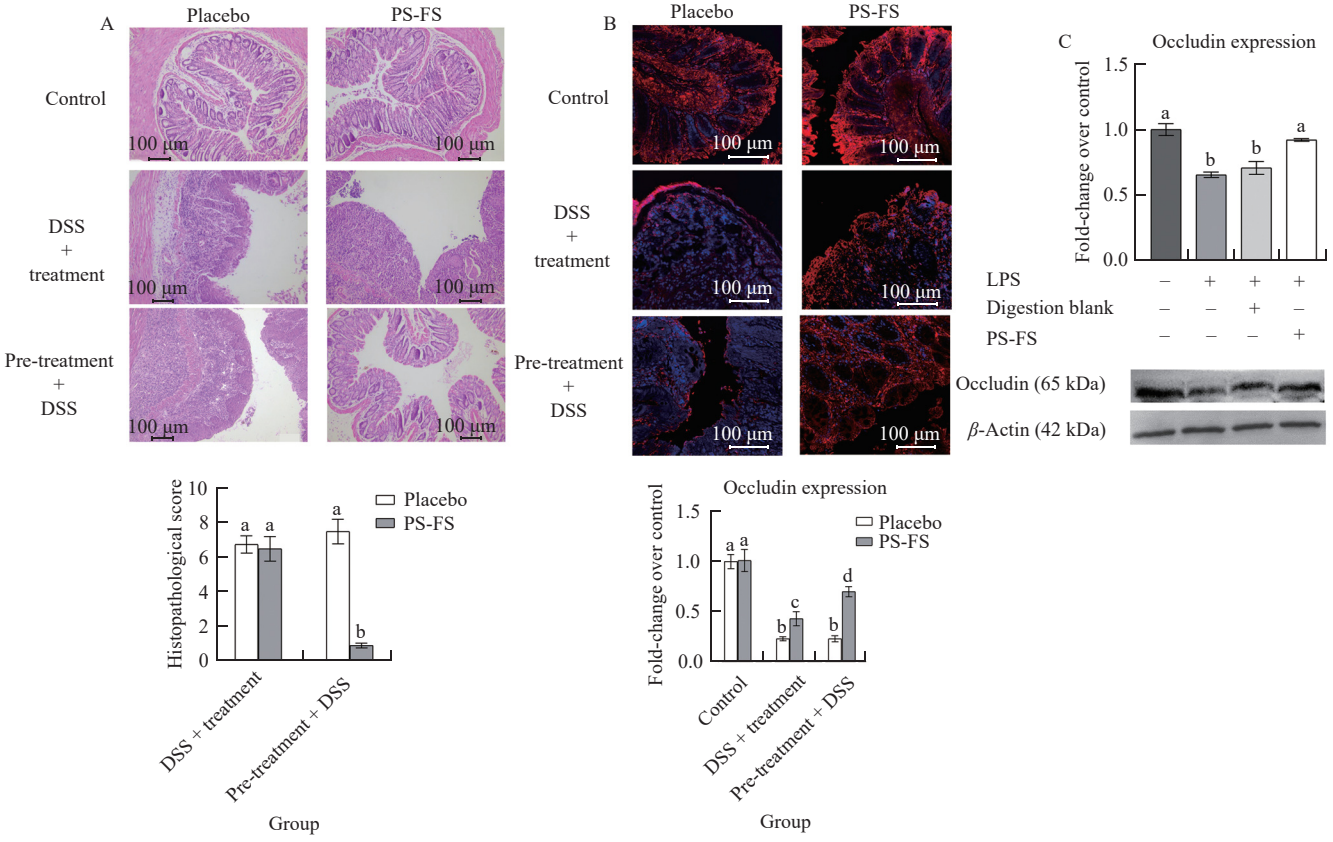

Fig. 5 (A) HE staining (10× magnification) and the corresponding histopathological score of colon tissue. Control mice did not manifest any histpathological damage and therefore data are not shown. (B) Immunofluorescent staining (20× magnification) of occludin (red) with DAPI nuclear-stain (blue) and the corresponding expression of occludin in colon tissue. (C) Occludin expression in Caco-2 cells in a bi-compartmental model of LPS-induced inflammatory stress in differentiated Caco-2 cells. Data are expressed as mean ± standard deviation. Different letters (a–d) indicate statistically significant difference ($P < 0.05$) between conditions.

benefits were provided by the pre-treatment, as it led to a significant recovery of colonic architecture, a reduction in the abundance of immune cells, and an improvement in the integrity of the intestinal barrier (3-fold increase in the expression of occludin *vs*. DSS + placebo, $P < 0.05$). In addition, the results of the *in vitro* study confirm the positive effect of PS-FS on the structure of the intestinal epithelium in terms of occludin expression in Caco-2 cells (Fig. 5C). In this context, exposure to BF of PS-FS mitigated the counterproductive impact of LPS on occludin expression, leading to an augmentation in its protein expression (by 29.6%) (*vs*. LPS + digestion blank). This result underscores the translational relevance of the co-culture system in capturing the effects that a treatment might exert on the structural components of the epithelium *in vivo*.

3.3 Regulation of the expression of inflammation biomarkers

Cytokine levels are the most used tissue biomarkers for the assessment of intestinal inflammation and its severity. Nevertheless, it is advisable to complement these analyses with non-invasive biomarkers (e.g., fecal Lnc-2) that allow monitoring the evolution of the disease over time. Furthermore, the involvement of oxidative stress in the etiopathogenesis of intestinal inflammation underlines the importance of evaluating biomarkers related to oxidative stress, such as MPO activity and ROS level. The results of the *in vivo* model show an increase in fecal content of Lcn-2, tissue levels of pro-inflammatory cytokines, and MPO activity, as well as a reduction in IL-10 levels, due to DSS exposure (Fig. 6). These changes were attenuated by PS-FS treatment and pre-treatment, presenting lower levels of Lcn-2 (by 29%–47% and 33%–36%, respectively), TNF-α (63% and 55%), and IL-6 (43% and 40%), as well a lesser MPO activity (15% and 30%), compared to placebo group. Likewise, PS-FS treatment and pre-treatment increased IL-10 levels (2.9- and 3.5-fold *vs*. DSS + placebo, respectively, $P < 0.05$). As was observed in other parameters (colon edematization, histopathology and occludin expression), pre-treatment with PS-FS seems to provide greater protection against inflammation compared to treatment, as deduced from the greater inhibition of the MPO activity (reaching values of healthy mice) and the greater increase in tissue levels of IL-10. Furthermore, the exposition to BF of PS-FS attenuated the LPS-induced secretion of TNF-α (9.3%), IL-6 (54%), and IL-8 (28.4%) in the *in vitro* model (Fig. 7). Along the same lines, exposure to PS-FS protected against oxidative stress, thus resulting in lower (by 46.5%) intracellular levels of ROS in Caco-2 cells (*vs*. LPS + digestion blank, $P < 0.05$).

3.4 Biochemistry pathway of anti-inflammatory effect of PS

Due to its importance in the immune response, NF-κB-COX-2-PGE_2 pathway was evaluated as a therapeutic target of PS, as previosly described with other bioactive compounds[32]. In this regard, the results of the *in vivo* study showed that treatment and pre-treatment with PS-FS significantly reduced (*vs*. DSS + placebo, $P < 0.05$) the expression of COX-2 (Fig. 8A). In the *in vitro* model, the inhibitory impact of PS-FS on COX-2 expression was substantiated, with a significantly reduction (by 44.1%) compared to LPS + digestion blank (Fig. 8B). Furthermore, it was demonstrated that this regulatory effect coincided with a decrease in the secretion of its primary product, PGE_2, in RAW264.7 cells (by 24.5%). Regarding the impact on the NF-κB p65 subunit, the administration of PS-FS led to a decrease in its phosphorylation within the mouse colon. This effect was further reinforced by the observation of diminished nuclear translocation of this subunit in RAW264.7 cells following exposure to the BF of PS-FS (by 34.5%).

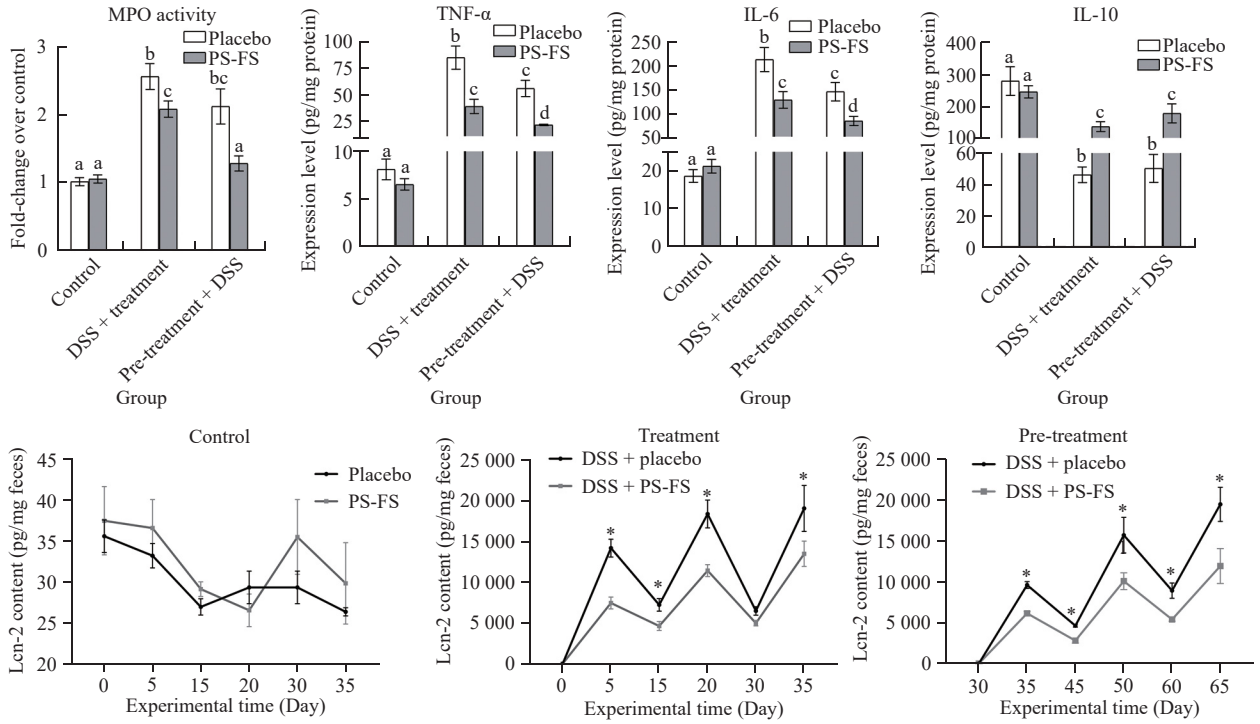

Fig. 6 MPO activity and expression of pro-(TNF-α and IL-6) and anti-inflammatory cytokines (IL-10) in colon tissue, and fecal concentration of Lcn-2. The administration of placebo or PS-FS started either with the first exposure to DSS (treatment) or 30 days before (pre-treatment). Different letters (a–d) or the asterisk indicate statistically significant difference ($P < 0.05$) between groups.

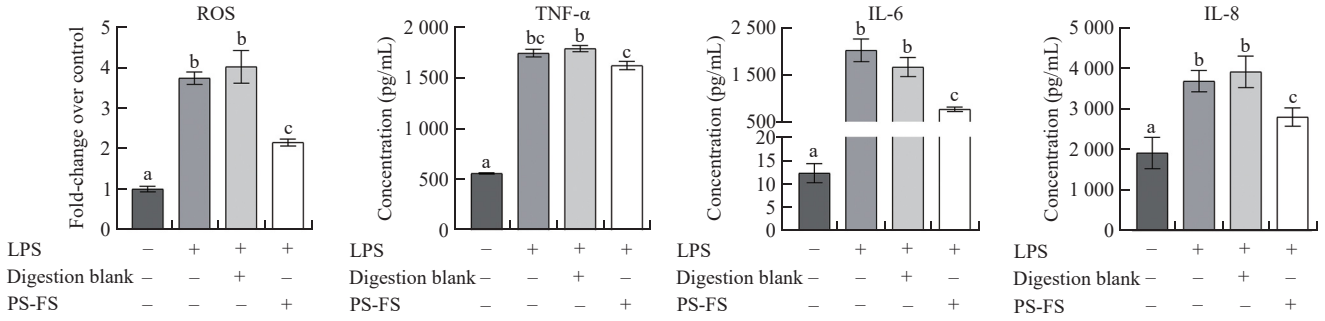

Fig. 7 Effect of BF of PS-FS on intracellular levels of ROS in Caco-2 cells and the secretion of pro-inflammatory cytokines in apical (IL-8) and basolateral (TNF-α and IL-6) medium in a bi-compartmental model of LPS-induced inflammatory stress in differentiated Caco-2 cells (apical) and RAW264.7 macrophage (basolateral). Data are expressed as mean ± standard deviation. Different letters (a–c) indicate statistically significant difference ($P < 0.05$) between conditions.

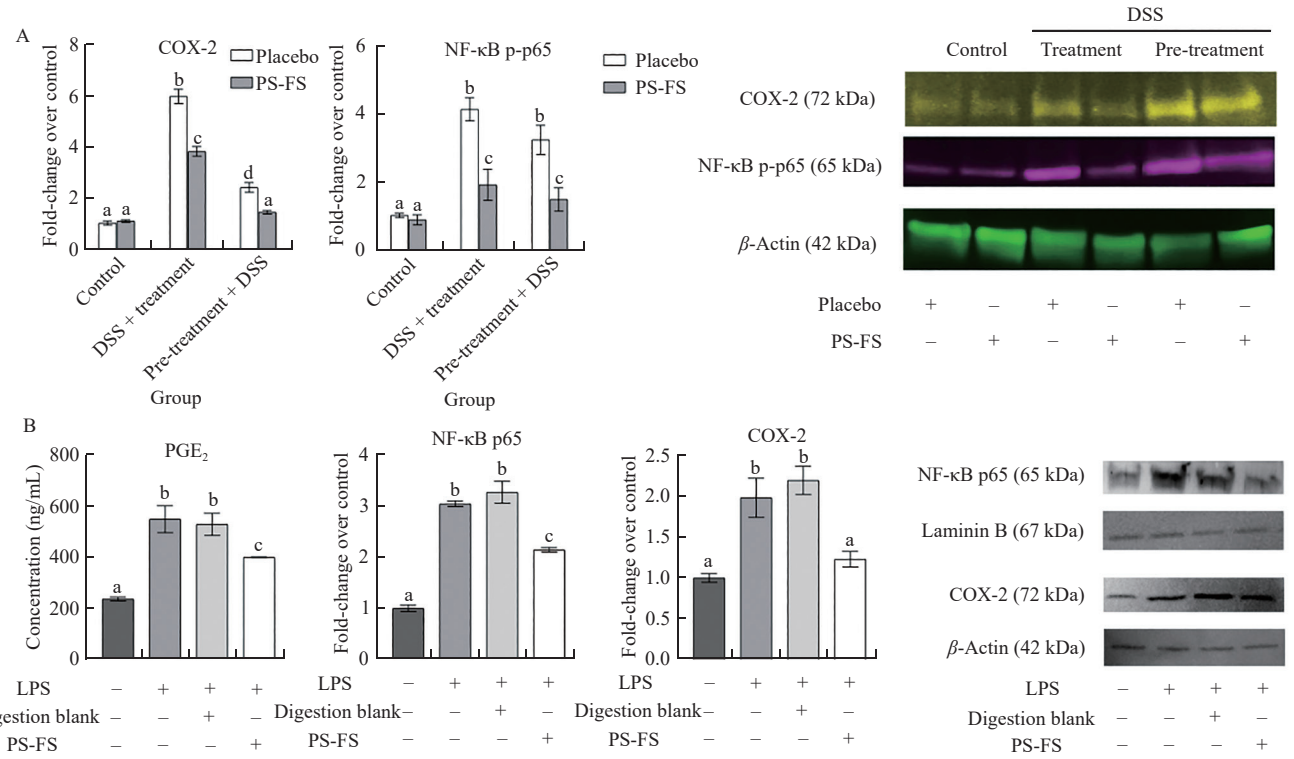

Fig. 8 (A) Relative expression of COX-2 and NF-κB p-p65 (normalized with *β*-actin) in colon tissue of control and DSS mice groups receiving placebo or PS-FS, from the time they were first exposed to DSS (treatment) or 30 days before (pre-treatment). (B) Expression of COX-2 (cytosolic fraction) and NF-κB p65 (nuclear fraction), normalized with *β*-actin (cytosolic) or laminin (nuclear), and secretion of PGE_2 in RAW264.7 cells in a bi-compartmental model of LPS-induced inflammatory stress in differentiated Caco-2 cells and RAW264.7 macrophages. Data are expressed as mean ± standard deviation. Different letters (a–d) indicate statistically significant difference ($P < 0.05$) between conditions.

4. Discussion

PS constitute a wide range of bioactive compounds known for their multiple health benefits. Among the widely documented effects is their ability to mitigate intestinal inflammation, as demonstrated by a large amount of *in vitro* research (with concentrations ranging from 0.01 to 250 μmol/L)[4-12] and animal experiments (using doses ranging from 10 and 100 mg/kg)[9-18]. However, aspects remain to be investigated, including their influence on the integrity of intestinal epithelial barrier function, which is significantly compromised in an inflammatory environment. This study employed a combined *in vivo* and *in vitro* approach to examine the anti-inflammatory properties of a PS-FS at the intestinal level. In terms of clinical symptoms, a decrease in rectal bleeding was noted, although no effect was observed in weight loss or diarrhea. Scientific literatures indicate that the protective effects of PS on clinical manifestations follow a dose-dependent pattern, specifically, doses of 35 mg/kg or a diet enriched with 0.4% PS demonstrate a reduction only in rectal bleeding[15-16], while higher doses (50 mg/kg or a diet enriched with 2% PS) exhibit protective effects against additional symptoms such as weight loss and loose stools[17-18]. Therefore, the dosage employed in this study (35 mg/kg) justifies the observed reduction only in rectal bleeding as a clinical symptom. Regarding the anatomopathological parameters evaluated in the animal model, the PS-FS showed a notable improvement in colon edema, in line with observations from previous studies[4,15]. Nevertheless, it was not observed an improvement in colonic shortening. It is noteworthy that a previous study consistently reported the ineffectiveness of PS in influencing

this parameter, although these authors identified positive changes in other inflammation-related biomarkers, in line with similar results reported in the current research[10].

Concerning biochemical parameters, a modulation in the levels of pro-inflammatory cytokines TNF-α, IL-6, and IL-8, as well as the anti-inflammatory cytokine IL-10, was observed. These findings are consistent with prior studies that have reported a decrease in the levels of pro-inflammatory cytokines (TNF-α, IL-1β, IL-2, IL-6, IL-8, and interferon γ) alongside an elevation in IL-10[4-6,9,11-17]. Regarding oxidative stress biomarkers, a decrease in MPO activity, a pro-oxidant enzyme involved in the immune response, was observed in the murine model. In the *in vitro* model, exposure to the BF of PS-FS resulted in an attenuation of the LPS-induced increase in intracellular ROS levels in Caco-2 cells. The antioxidant effect of PS in inflammation models has been previously documented, demonstrating a reduction in MPO activity and ROS levels, as well as an improvement in antioxidants defense, such as glutathione and antioxidant enzymes[6-8,12,17]. One of the signaling pathways involved in the inflammatory process and identified as one of the main molecular targets of PS is the NF-κB-COX-2-PGE_2 pathway. Within this cascade, the enzymatic activity of COX-2 leads to the generation of the pro-inflammatory mediator PGE_2[33]. Subsequently, this product triggers a signaling cascade that culminates in the activation of NF-κB transcription factors, among which the p65 and p50 subunits stand out. While residing in the cytoplasm, NF-κB remains inactive due to its association with the inhibitor of NF-κB (IκB). The activation cascade begins with the phosphorylation and activation of IκB kinase (IKK), which, in turn, phosphorylates IκB. Phosphorylation of IκB causes its degradation, releasing NF-κB subunits, which can undergo post-translational modifications (e.g., phosphorylation) and translocate to the nucleus, where they exert their biological activity[34]. Previous studies demonstrate an inhibition of the NF-κB-COX-2-PGE_2 pathway by PS, down-modulating different points: a) activity or phosphorylation of IKK[10,12,17]; b) phosphorylation and/or degradation of IκB[4,10,12,17]; c) phosphorylation, nuclear translocation and/or activity of p65[4,6-7,10,12,15,17,19]; d) expression of COX-2[1,6-7]; and e) PGE_2 production[7]. These findings were reproduced in the present study, revealing an inhibition in COX-2 expression and a decrease in PGE_2 production. Furthermore, there was a reduction in the phosphorylation of NF-κB p65, accompanied by a decrease in its nuclear translocation. Fig. 9 summarizes the biochemical mechanism through which PS mitigates inflammation.

Beyond reproducing the anti-inflammatory effects of PS described above, new findings were reported. Among the most notable is the restoration of tight junctions in the intestinal epithelium. This improvement was reflected in less histopathological damage and higher expression of the tight junction protein occludin, observed by immunofluorescence and Western blot assays. On the other hand, monitoring the non-invasive biomarker Lcn-2 throughout the assay revealed that the anti-inflammatory effect of PS begins in the early stages of colitis. In particular, these effects are manifested in the first week of treatment, as observed in the animal model of DSS-induced colitis, where a reduction in the secretion of this biomarker occurs in the first cycle of exposure to DSS. On the other hand, the efficacy of PS-FS to mitigate intestinal inflammation in the murine model was evaluated using two approaches: administering the product simultaneously with exposure to DSS and using a pre-treatment protocol, where PS-FS was administered 30 days before the first cycle and administration was continued until the end of the study. The results of the study revealed that pre-treatment showed superior benefits in terms of protection against inflammation compared to treatment. This fact suggests that the anti-inflammatory effect of PS may follow two potential mechanisms: a) act as a regulator of the immune response in a pro-inflammatory environment, and/or b) reinforce defense mechanisms in healthy conditions to reduce the inflammatory response to subsequent exposure to pro-inflammatory agents. The preventive effectiveness of PS may be associated with its capacity to enhance the antioxidant mechanisms, as described previosly[2]. Through the strengthening of these mechanisms, PS plays a crucial role in reducing the potential damage induced by ROS, ultimately serving to prevent issues related to oxidative stress, such as IBD. The preventive potential of PS described in this work opens new avenues of research and lays the foundation for possible clinical applications, particularly in people who are at higher risk of developing intestinal inflammation, beyond its therapeutic applications.

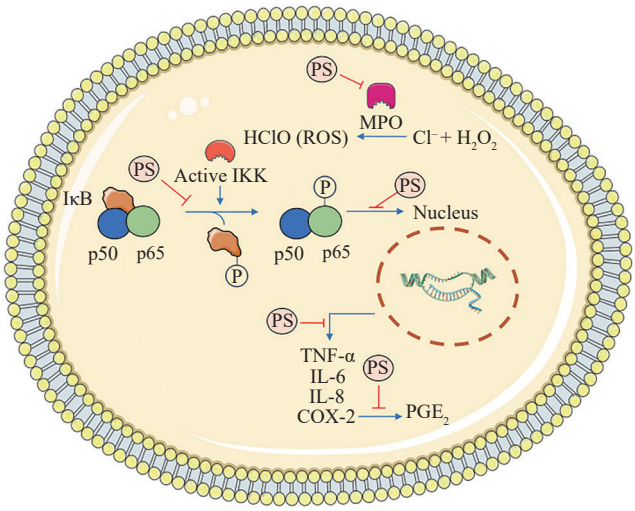

Fig. 9 PS demonstrate in *in vivo* and *in vitro* models of intestinal inflammation their ability to diminish the activity of the pro-oxidant enzyme MPO and the production of ROS. Additionally, they exhibit inhibitory effects on the phosphorylation of the NF-κB p65 subunit, preventing its nuclear translocation. This results in a reduction in the expression of pro-inflammatory cytokines (TNF-α, IL-6, and IL-8) and the enzyme COX-2, accompanied by a simultaneous decrease in its enzymatic product PGE_2.

In vitro models of intestinal inflammation serve as valuable tools to evaluate the anti-inflammatory properties of foods and their components[35]. However, a concern arises as results derived from these models are frequently not compared to results obtained from *in vivo* studies, calling into question their predictive accuracy. The reliability of *in vitro* models depends on their ability to replicate key aspects of the inflammatory response observed in living organisms, making animal models indispensable for validation purposes. To address this question, this study evaluated the anti-inflammatory effects of PS using an *in vitro* model based on co-culture of intestinal Caco-2 cells and RAW264.7 macrophages. In order to verify the results obtained, they were compared with those derived from an *in vivo* model of DSS-induced colitis. In this aspect, a notable correlation was identified between the results of both models, which validates the reliability of the *in vitro* model. This is particularly significant as it underlines the applicability of the *in vitro* model in evaluating the ability of a food product to modulate inflammatory responses. In this way, the results of this study ensure that

the conclusions drawn from studies on the anti-inflammatory activity of food products are reliable and can be applied with confidence to clinical scenarios. Additionally, the consistent outcomes observed in both *in vivo* and *in vitro* models may suggest a null involvement of colonic microbiota on the anti-inflammatory activity of PS. However, complete exclusion cannot be guaranteed, since a metabolite resulting from colonic fermentation of *β*-sitosterol have shown anti-proliferative effects in an *in vitro* colon cancer model[25]. Consequently, it is pertinent to investigate its potential anti-inflammatory activity in future studies.

Conflict of interest

The authors declare no conflict of interest.

Acknowledgements

This study is part of the project PID2019-104167RB-I00 funded by MCIN/AEI/10.13039/501100011033 and Generalitat Valenciana (CIAICO/2021/076). Mussa Makran holds an FPU19/00156 grant from the Ministry of Sciences, Innovation and Universities (Spain).

Ethical Statement

The animal study was approved by the Generalitat Valenciana, Spain (protocol code 2022/VSC/PEA/0256, date November 10, 2022).

Data Availability Statement

The data presented in this study are available on request from the corresponding author.

References

[1] G.P. Ramos, K.A. Papadakis, Mechanisms of disease: inflammatory bowel diseases, Mayo Clin. Proc. 94 (2019) 155-165. https://doi.org/10.1016/j.mayocp.2018.09.013.

[2] W.A. Rose, K. Sakamoto, C.A. Leifer, Multifunctional role of dextran sulfate sodium for *in vivo* modeling of intestinal diseases, BMC Immunol. 13 (2012) 1-13. https://doi.org/10.1186/1471-2172-13-41.

[3] B. Salehi, C. Quispe, J. Sharifi-Rad, et al., Phytosterols: from preclinical evidence to potential clinical applications, Pharmacol. 11 (2021) 599959. https://doi.org/10.3389/fphar.2020.599959.

[4] M. Valerio, A.B. Awad, *β*-Sitosterol down-regulates some pro-inflammatory signal transduction pathways by increasing the activity of tyrosine phosphatase SHP-1 in J774A. 1 murine macrophages, Int. Immunopharmacol. 11 (2011) 1012. https://doi.org/10.1016/j.intimp.2011.02.018.

[5] G. López-García, A. Cilla, R. Barberá, et al., Anti-inflammatory and cytoprotective effect of plant sterol and galactooligosaccharides-enriched beverages in Caco-2 cells, J. Agric. Food Chem. 68 (2020) 1862. https://doi.org/10.1021/acs.jafc.9b03025.

[6] I.A. Lee, E.J. Kim, D.H. Kim, Inhibitory effect of *β*-sitosterol on TNBS-induced colitis in mice, Planta Med. 78 (2012) 896-898. https://doi.org/10.1055/s-0031-1298486.

[7] J.J. Moreno, Effect of olive oil minor components on oxidative stress and arachidonic acid mobilization and metabolism by macrophages RAW264.7, Free Radic. Biol. Med. 35 (2003) 1073-1081. https://doi.org/10.1016/S0891-5849(03)00465-9.

[8] M. Vivancos, J. J. Moreno, *β*-Sitosterol modulates antioxidant enzyme response in RAW264.7 macrophages, Free Radic. Biol. Med. 39 (2005) 91-97. https://doi.org/10.1016/j.freeradbiomed.2005.02.025.

[9] A. Mencarelli, B. Renga, G. Palladino, et al., The plant sterol guggulsterone attenuates inflammation and immune dysfunction in murine models of inflammatory bowel disease, Biochem. Pharmacol. 78 (2009) 1214-1223. https://doi.org/10.1016/j.bcp.2009.06.026.

[10] J.H. Cheon, J.S. Kim, J.M. Kim, et al., Plant sterol guggulsterone inhibits nuclear factor-κB signaling in intestinal epithelial cells by blocking IκB kinase and ameliorates acute murine colitis, Inflamm. Bowel Dis. 12 (2006) 1152-1161. https://doi.org/10.1097/01.mib.0000235830.94057.c6.

[11] Y. Ding, H.T. Nguyen, S.I. Kim, et al., The regulation of inflammatory cytokine secretion in macrophage cell line by the chemical constituents of *Rhus sylvestris*, Bioorg. Med. Chem. Lett. 19 (2009) 3607-3610. https://doi.org/10.1016/j.bmcl.2009.04.129.

[12] K.A. Kim, I.A. Lee, W. Gu, et al., *β*-Sitosterol attenuates high-fat diet-induced intestinal inflammation in mice by inhibiting the binding of lipopolysaccharide to toll-like receptor 4 in the NF-κB pathway, Mol. Nutr. Food Res. 58 (2014) 963-972. https://doi.org/10.1002/mnfr.201300433.

[13] A.S. Awaad, R.M. El-Meligy, N.A. Al-Jaber, et al., Anti-ulcerative colitis activity of compounds from *Euphorbia granuleta* Forssk, Phytother. Res. 27 (2013) 1729-1734. https://doi.org/10.1002/ptr.4985.

[14] R. Aldini, M. Micucci, M. Cevenini, et al., Antiinflammatory effect of phytosterols in experimental murine colitis model: prevention, induction, remission study, PLoS ONE 9 (2014) e108112. https://doi.org/10.1371/journal.pone.0108112.

[15] G. López-García, A. Cilla, R. Barberá, et al., Effect of a milk-based fruit beverage enriched with plant sterols and/or galactooligosaccharides in a murine chronic colitis model, Foods 8 (2019) 114. https://doi.org/10.3390/foods8040114.

[16] S. Feng, Z. Dai, A. Liu, et al., *β*-Sitosterol and stigmasterol ameliorate dextran sulfate sodium-induced colitis in mice fed a high fat Western-style diet, Food Funct. 8 (2017) 4179-4186. https://doi.org/10.1039/C7FO00375G.

[17] M.S. Islam, T. Murata, M. Fujisawa, et al., Anti-inflammatory effects of phytosteryl ferulates in colitis induced by dextran sulphate sodium in mice, Br. J. Pharmacol. 154 (2008) 812-824. https://doi.org/10.1038/bjp.2008.137.

[18] A.A. te Velde, F. Brüll, S.E.M. Heinsbroek, et al., Effects of dietary plant sterols and stanol esters with low- and high-fat diets in chronic and acute models for experimental colitis, Nutrients 7 (2015) 8518-8531. https://doi.org/10.3390/nu7105412.

[19] D.S. Doke, S.C. Dhawale, Alternatives to animal testing: a review, Saudi Pharm. J. 23 (2015) 223-229. https://doi.org/10.1016/j.jsps.2013.11.002.

[20] G. López-García, A. Alegría, R. Barberá, et al., Antiproliferative effects and mechanism of action of phytosterols derived from bioactive plant extract, in: M.F. Ullah, A. Ahmad (Eds.), Nutraceuticals and natural product derivatives: disease, prevention & discovery, Wiley-Blackwell, Hoboken, USA, 2018, 145-165. https://doi.org/10.1002/9781119436713.ch7.

[21] T. Tanoue, Y. Nishitani, K. Kanazawa, et al., *In vitro* model to estimate gut inflammation using co-cultured Caco-2 and RAW264.7 cells, Biochem. Biophys. Res. Commun. 374 (2008) 565-569. https://doi.org/10.1016/j.bbrc.2008.07.063.

[22] B. Chassaing, J.D. Aitken, M. Malleshappa, et al., Dextran sulfate sodium (DSS)-induced colitis in mice, Curr. Protoc. Immunol. 104 (2014) 15.25.1-15.25.14. https://doi.org/10.1002/0471142735.im1525s104.

[23] M. González-Larena, G. García-Llatas, M.C. Vidal, et al., Stability of plant sterols in ingredients used in functional foods, J. Agric. Food Chem. 59 (2011) 3624-3631. https://doi.org/10.1021/jf1044102.

[24] M. Makran, N. Faubel, G. López-García, et al., Sterol bioaccessibility in a plant sterol-enriched beverage using the INFOGEST digestion method: Influence of gastric lipase, bile salts and cholesterol esterase, Food Chem. 382 (2022) 132305. https://doi.org/10.1016/j.foodchem.2022.132305.

[25] M. Makran, G. Garcia-Llatas, A. Alegría, et al., Ethylcoprostanol modulates colorectal cancer cell proliferation and mitigates cytotoxicity of cholesterol metabolites in non-tumor colon cells, Food Funct. 14 (2023) 10829-10840. https://doi.org/10.1039/D3FO01868G.

[26] B. Chassaing, G. Srinivasan, M.A. Delgado, et al., Fecal lipocalin 2, a sensitive and broadly dynamic non-invasive biomarker for intestinal inflammation, PLoS ONE 7 (2012) e44328. https://doi.org/10.1371/journal.pone.0044328.

[27] H.S. Cooper, S.N. Murthy, R.S. Shah, et al., Clinicopathologic study of dextran sulfate sodium experimental murine colitis. Lab. Investig. 69 (1993) 238-249.

[28] J. Peng, J. Leng, H. Tian, et al., Geniposide and chlorogenic acid combination ameliorates non-alcoholic steatohepatitis involving

the protection on the gut barrier function in mouse induced by high-fat diet, Front. Pharmacol. 9 (2018) 1399. https://doi.org/10.3389/fphar.2018.01399.

[29] P.P. Bradley, D.A. Priebat, R.D. Christensen, et al., Measurement of cutaneous inflammation: estimation of neutrophil content with an enzyme marker, J. Investig. Dermatol. 78 (1982) 206-209. https://doi.org/10.1111/1523-1747.ep12506462.

[30] I. Restivo, M.G. Basilicata, I.C. Giardina, et al., A combination of polymethoxyflavones from *Citrus sinensis* and prenylflavonoids from *Humulus lupulus* counteracts IL-1β-induced differentiated Caco-2 cells dysfunction via a modulation of NF-κB/Nrf2 activation, Antioxidants 12 (2023) 1621. https://doi.org/10.3390/antiox12081621.

[31] M. M. Bradford, A rapid and sensitive method for the quantitation of microgram quantities of protein utilizing the principle of protein-dye binding, Anal. Biochem. 72 (1976) 248-254. https://doi.org/10.1016/0003-2697(76)90527-3.

[32] K. Lin, Y. Wang, J. Gong, et al., Protective effects of total flavonoids from *Alpinia officinarum rhizoma* against ethanol-induced gastric ulcer *in vivo* and *in vitro*, Pharm. Biol. 58 (2020) 854-862. https://doi.org/10.1080/13880209.2020.1803370.

[33] I.L. Bonta, M.J. Parnham, Prostaglandins and chronic inflammation, Biochem. Pharmacol. 27 (1978) 1611-1623. https://doi.org/10.1016/0006-2952(78)90169-7.

[34] S. Giridharan, M. Srinivasar, Mechanisms of NF-κB p65 and strategies for therapeutic manipulation, Inflamm. Res. 11 (2022) 407-419. https://doi.org/10.2147/JIR.S140188.

[35] M.D.C. Ponce de León-Rodríguez, J.P. Guyot, C. Laurent-Babot, Intestinal *in vitro* cell culture models and their potential to study the effect of food components on intestinal inflammation, Crit. Rev. Food Sci. Nutr. 59 (2019) 3648-3666. https://doi.org/10.1080/10408398.2018.1506734.